Shape instability of a biomembrane driven by a local softening of the underlying actin cortex

A. Boulbitch,[1,*] R. Simson,[1] D. A. Simson,[1] R. Merkel,[1] W. Häckl,[2] M. Bärmann,[1] and E. Sackmann[1]
[1]*Department of Biophysik E22, TU München, James-Franck-Strasse, D-85747 Garching bei München, Germany*
[2]*Thannenthal 27 1/2, D-84367 Zeilarn, Germany*

(Received 9 February 1999; revised manuscript received 13 December 1999)

We present a theory showing that local shape instabilities of composite biological membranes, consisting of a lipid bilayer and an underlying actin cortex, can be triggered by a local softening of the membrane-associated cytoskeleton. A membrane containing such cortical defects can form blisters or invaginations, depending on external conditions. The theoretical predictions agree with observations provided by two sets of experiments: (i) microscopic observations of shape changes of giant vesicles with underlying shells of a thin actin network show the formation of local blisters and (ii) micropipet aspiration experiments of *Dictyostelium discoideum* cells in which we observed the formation of blisters in the aspirated cell part. In the latter experiments, the existence of a hole in the underlying cortex is confirmed by observation of the entrance of cell organelles into the blister. Our model may also be applied to the formation of lobopodia, fast-growing cell protrusions that play an important role in the locomotion and spreading of biological cells.

PACS number(s): 87.16.−b, 87.19.Rr

I. INTRODUCTION

This paper describes a mechanical model of the surface protrusions of biological cells. Every mechanical model of a cell has to take into account the cell's morphology. A biological cell exhibits a layered architecture. The outermost layer is the fluid mosaic membrane as described by Singer and Nicolson [1]. It consists of a compound material of phospholipids and membrane proteins and shows a thickness of some nanometers. In parenchymal animal cells (i.e., tissue cells such as liver cells), on which we will focus for the rest of the paper, the plasma membrane carries an additional thin layer of polyelectrolytes at the outside called the glycocalix. This fluid mosaic membrane exhibits the properties of a two-dimensional fluid [2].

In close proximity to the fluid mosaic membrane a second layer, the cortex, follows [3–5]. In most cases, it contains high concentrations of microfilaments (i.e., filamentous actin) and crosslinking proteins. This layer has a gel-like consistency and is very thin compared to the size of the cell. It is tightly coupled to the fluid mosaic membrane by colloidal interactions (e.g., electrostatics) and, most importantly, by specific binding between integral membrane proteins and cortical proteins. From the point of view of mechanics, cortex and membrane usually behave as one layer, from now on termed the ''compound membrane.'' The fluid mosaic membrane serves as a barrier, controlling osmotic pressure and surface potential, whereas the actin cortex endows the compound membrane with mechanical stiffness (i.e., solidlike properties).

The core of the cell is filled with cytoplasm and organelles. The cytoplasm also contains cytoskeletal structures that contribute to the mechanical behavior of the cell. However, in the cells considered here, the density of polymers in the cytoplasm is greatly reduced as compared to the cortex.

Many of the essential functions of biological cells (e.g., engulfing food, spreading on substrates, and locomotion) require the formation of surface protrusions [6–8]. These protrusions exhibit very different shapes, speeds, and mechanical properties [6,7]. Therefore it is extremely unlikely that they are all caused by a single underlying mechanism. In this paper we will focus on blebs, also called lobopodia. This type of cell protrusion is the most rapidly extending one. The formation of lobopodia is common for healthy cells and plays an important role in cell spreading on substrates and cell locomotion. The formation of lobopodia has been extensively studied for locomoting blebbing Walker carcinosarcoma cells [9,10], melanoma cell lines lacking actin-binding proteins [11,12], and locomoting *Amoeba proteus* [13].

On living cells, lobopodia (blebs) develop in a few seconds. Therefore the initial stages of bleb growth are rarely seen. The shape of a well-developed bleb is close to a spherical cap. Later on we will show that this is not the case in the very first stage of lobopodium growth. Growing blebs contain no filamentous actin. Their growth can be triggered by intracellular pressure [10,14]. Together with their spherical shape and their rapid growth, this shows that bleb formation is driven by pressure, either hydrostatic or osmotic. The volume of a bleb increases linearly in time until the growth suddenly stops. Interruption of bleb growth occurs due to the formation of a new cortical structure lining the bleb's membrane, i.e., polymerization of actin at the membrane [6,9,12,13]. Most importantly, the cortex and fluid mosaic membrane split during bleb growth. Blebs grow at locations where the cortex is weakened (for a sketch of this process see Fig. 1). This was shown by immunofluorescence techniques for Walker carcinosarcoma cells [9] and by genetic techniques for melanoma cells [11]. After the initialization at a weak spot of the cortex, blebs can grow by two different modes. Either the base of the bleb (i.e., the area where the ''old'' cortex is separated from the fluid mosaic membrane) grows or it remains constant. In the first case, the cortex is successively peeled off the membrane [see Fig. 1(c)]. This

*Author to whom correspondence should be addressed.
FAX: 49(89) 2891-2469.
Electronic address: aboulbit@physik.tu-muenchen.de

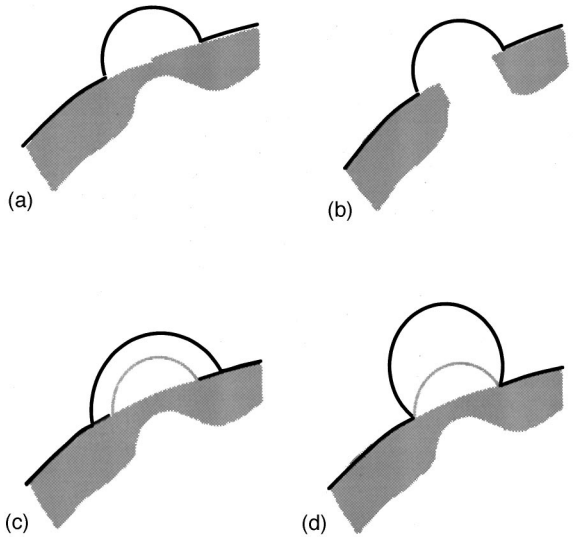

FIG. 1. Sketches of the formation of lobopodia (blebs). The gray areas symbolize the cortex, the heavy lines the fluid mosaic membrane. The gray lines represent the fluid mosaic membrane at a previous instant. (a) Growth at a location where the cortex is weakened. (b) Growth at a cortical hole. (c) Bleb expansion by successive pealing; i.e., the base of the bleb grows. (d) Bleb expansion by successive inflation; i.e., the base of the bleb remains stationary.

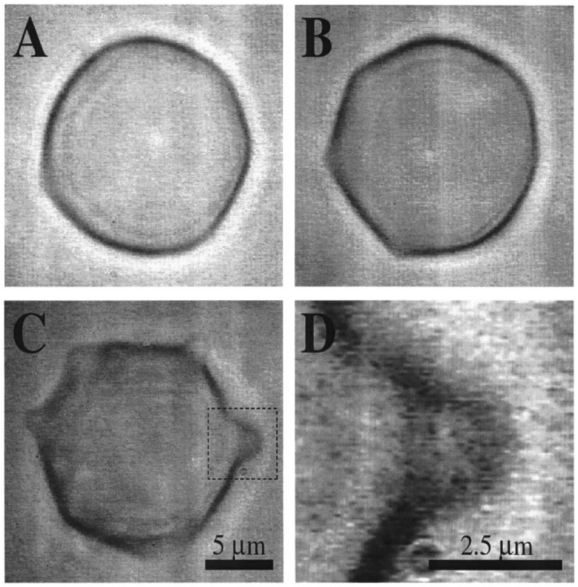

FIG. 2. Phase-contrast micrograph of an actin-containing vesicle at three different temperatures: (A) at 26.0 °C, (B) at 26.7 °C, and (C) at 32.8 °C. Image (D) shows an enlargement of a protrusion shown in image (C) (dotted frame). The blister demonstrates manifested fluctuations seen as the blurred image of the membrane.

happens in *Amoeba proteus* [13]. In the latter case, the fluid mosaic membrane flows with respect to the cortex [15] to allow a continuous ''inflation'' of the bleb [see Fig. 1(d)]. This takes place in melanoma cells devoid of filamin, a major actin cross-linking protein [12].

The initial phase of bleb development is a very intriguing process on which this paper is focused. Here we report the observation of blister formation in regions where the submembraneous cytoskeleton exhibits a local softening in actin-filled vesicles and *Dictyostelium* cells. We show theoretically that a local softening of the cytoskeleton necessarily gives rise to an instability of the membrane shape.

The paper is organized as follows. We report our experimental observations of local shape changes of the membranes of giant vesicles with reconstituted actin shells in Sec. II A, and of *Dictyostelium* cells in Sec. II B. In Sec. III A we present a general theoretical study of the problem. We introduce a function describing the local softening and deduce a basic equation that has to be solved to determine the local shape instability arising from local softening. We give a complete description of the membrane instability and overcritical behavior assuming that the solution of this equation is found. In Appendixes A–D, we present exact and approximate solutions of the basic equations for different types of soft regions. In Sec. IV we discuss our results and their applicability to phenomena observed after the poisoning of liver cells with phalloidin or cytochalasin B, two alcaloids acting specifically on the actin cytoskeleton. In this example, the formation of blebs and invaginations is observed depending on the experimental conditions. This can be easily described by our theoretical model.

II. LOCAL SHAPE INSTABILITIES DRIVEN BY DEFECTS IN ARTIFICIAL AND NATURAL ACTIN CORTICES: EXPERIMENTS

A. Local shape instabilities in actin-filled vesicles

Vesicles filled with polymerized filamentous actin, which forms a thin shell beneath the inner leaflet (cortex), provide a model system allowing us to study the mechanical properties of cell membranes. The method of preparation of the actin-filled vesicles and their mechanical properties are reported elsewhere [16,17]. Giant vesicles (diameter 5–20 μm) were prepared from dimyristoylphosphatidylcholine (DMPC) containing 2.5 mol % of the Mg^{2+} (Ca^{2+}) ionophore A-23187 in a solution of monomeric actin at a temperature of 30 °C, i.e., well above the main transition temperature of DMPC of about 24 °C. Polymerization of actin was induced by 2 mM $MgCl_2$, the Mg^{2+} ions being transported into the vesicles via the ionophore. Polymerization of external actin was suppressed by DNAase I, an enzyme binding with high specificity to monomeric actin, thus preventing the polymerization. The actin-containing vesicles were then observed by phase-contrast microscopy on a thermostated stage. Filamentous actin concentrated beneath the lipid bilayer, as was demonstrated with fluorescent-labled actin (data are not shown here).

A slight increase in the temperature (by 1 to 2 °C) led to the formation of blisters protruding from the surface. Figures 2(a)–2(c) show successive shapes of such a vesicle during the temperature increase. Figure 3(a) shows a typical phase-contrast micrograph of the complete equatorial contour of another vesicle. One can clearly distinguish flattened regions, which exhibit a dark contour, from blisters exhibiting only a faint contour. Observations of video sequences show that the

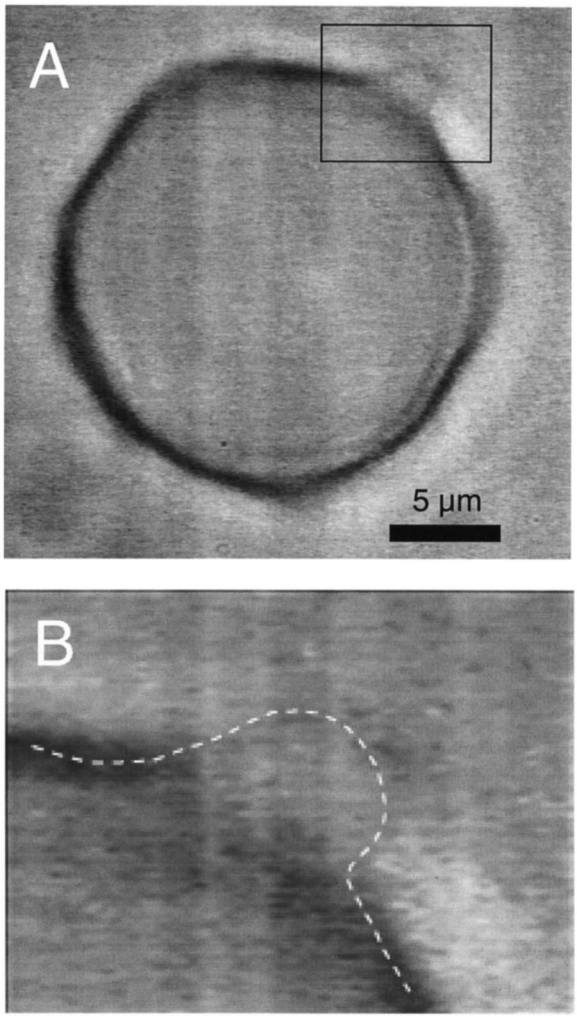

FIG. 3. Actin-containing giant phospholipid vesicle as seen by phase-contrast video microscopy. Actin concentration was 7 μM. Vesicles were produced as described in the text. (A) Overview: a whole vesicle focused in the equator level. The box marks the area that is shown enlarged below. (B) Detail showing the contour of one of the blisters protruding from the vesicle shown in (A). The white trace was drawn with respect to the dynamic fluctuations of the blister membrane clearly seen on the video record.

dark regions are relatively stiff, whereas the contours of the blisters are strongly fluctuating. Both observations, microscopic contrast and membrane fluctuations, indicate that the membrane is attached to the ''cortex'' in the flattened regions, whereas it is not supported by a cortex in the blister regions. In Fig. 2(d) and 3(b), one blister is enlarged, showing that below the membrane protrusion, the dark contour of the composite actin/membrane cortex is interrupted. This is considered to be a local defect (possibly a cortex hole) in the theory developed below. Note that this type of temperature-induced shape change differs drastically from the shape transformations observed experimentally for pure DMPC vesicles and described theoretically [18].

B. Local shape instability driven by a defect in the actin cortex of a cell plasma membrane during micropipet aspiration of *Dictyostelium discoideum* cells

In this set of experiments, we studied the local deformations of amoebalike cells of the slime mold *Dictyostelium*

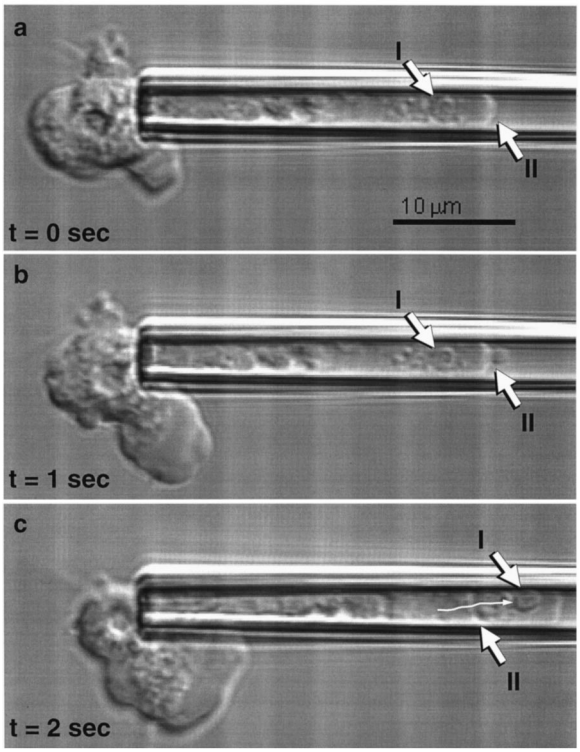

FIG. 4. A wild-type AX2 *Dictyostelium* cell, observed with differential interference contrast microscopy, has been aspirated with a glass micropipet at the cell front (II). Frequently, formation of small spherical protrusions occurred in the pipet, here at a suction pressure of 1000 Pa (a). The arrows denote the position of a certain cell organelle within the aspirated cell part (I). The transient formation of a spherical blister can be observed in (b). These blisters grow rapidly until eventually a new stable cell front is formed (c). Blisters always appear at the site of a defect in the actin cortex of the cell membrane. While the defect itself cannot be seen, its existence is clear from the fact that the influx of organelles into the newly formed protrusion is confined to a small pore. The white line in (c) marks the path taken by the organelle (I). As this organelle is bigger than the formed pore, the organelle obstructs the pore for a while before it can squeeze through. Note that the actin cortex remains visible at the old position of the cell front (c, II).

discoideum by aspiration with glass micropipets (cf [19,20] for details about *Dictyostelium* cells). Cylindrical glass micropipets have been used routinely for determining properties of blood cells or lipid vesicles (for a review of the micropipet aspiration technique, see [21]). The pipet was connected to a water manometer, allowing us to apply well-defined suction pressures to the cell. In this study, we used pipets with an inner diameter of about 4 μm, which is small compared to the typical diameter of *Dictyostelium* cells, which is about 15 μm. Cells were cultivated on standard medium agar plates using *Klebsiella aerogenes* as a bacterial food source, and were treated as previously described [22].

Suction pressures of about 800 Pa were used to aspirate parts of the cell membrane and the cytoplasm [Fig. 4(a)]. Frequently, cells responded to the applied suction pressure in a stepwise manner where the repeated formation of small spherical protrusions could be observed. These protrusions expanded within fractions of a second to fill the whole pipet diameter, leading to a sudden increase in the length of the aspirated cell part. The shape of these protrusions remained

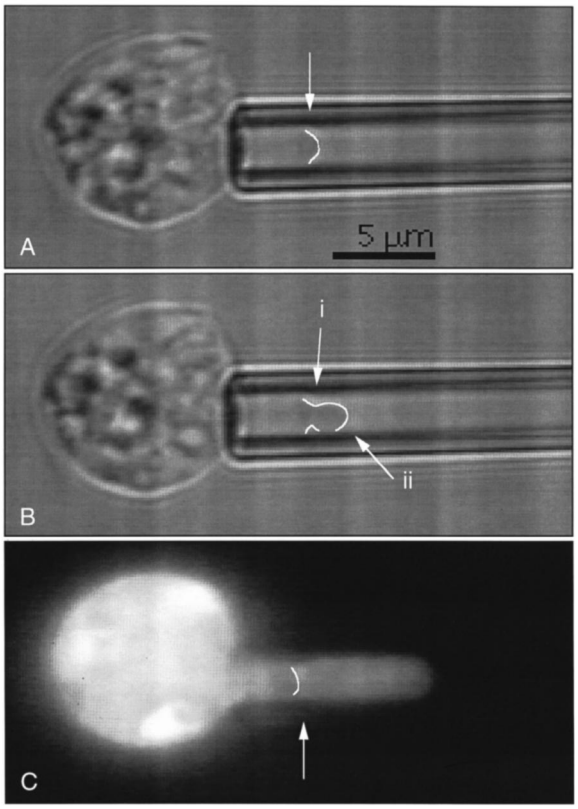

FIG. 5. Shown is the formation of a protrusion for an aspirated mutant cell of *Dictyostelium discoideum* containing GFP-labeled actin. (A) The cell aspirated into the micropipet. The arrow indicates the cap of the aspirated part. (B) The cell after formation of the small bleblike protrusion in conventional microscopy (as that shown in Fig. 4); (i) the cap, (ii) the protrusion. (C) shows the image of the same cell in fluorescence microscopy. Bright regions denote high actin concentrations. A bright band (arrow) is visible at the base of the newly formed protrusion, indicating the existence of a cortical structure at this position. The white traces were drawn beneath the lighter region of the image representing the membrane clearly seen on the video record.

spherical throughout the growth process. Protrusion formation occurred at different sites of the front cap of the aspirated part of the cell [Fig. 4(b) shows formation of the protrusion in the middle of the cap]. This suggests that some local weakening of the internal structure of the composite cell membrane determines the formation and location of the protrusions. Most likely, the weakened structure is the membrane-associated actin cortex and the protrusions are formed above defects in the actin shell. In some experiments we observed the influx of organelles into an emerging protrusion. An example is shown in Figs. 4(b) and 4(c). This suggests that the cortical defects are in most cases small cortical pores located right at the base of the protrusion. Additional evidence for this notion is provided by fluorescence studies using mutant *Dictyostelium* cells that contain actin that was genetically fused with a green fluorescent protein (GFP). Using a fluorescence microscope, high concentrations of actin such as cortical structures show up as bright regions against the darker background in these mutant cells. Figure 5 shows the formation of a protrusion for a GFP mutant cell; Figs. 5(a) and 5(b) show the cell in differential interference microscopy before and after the protrusion has formed. Figure 5(c) shows the same cell in fluorescence microscopy about 1 sec after 5(b). One can clearly identify a bright band at the position marked by the arrow. This indicates that there is indeed a cortical structure at the position from which the protrusion originated, and that splitting of the fluid mosaic membrane and actin cortex occurred.

Our observations imply that blisters grow from cortical defects. The process closely resembles the formation of lobopodia in undisturbed cells. Therefore it may be described as aspiration-induced formation of lobopodia or blebs.

III. THEORETICAL DESCRIPTION OF LOCAL SHAPE INSTABILITIES OF THE CELL MEMBRANE

The animal cell membrane represents a composite shell composed of extracellular polymers, a lipid bilayer, and an actin cortex. We focus on the bilayer and the cortex since they play an important role in the stability of the cell shape. Strong attraction between these two subshells (driven by nonspecific forces and integral membrane proteins specifically binding to cortex components) provides the integrity of the composite membrane, which is very important for its biological functions. Detachment of the bilayer from the cortex demands either very high local mechanical loads (as take place, for example, under tether formation) or the application of biochemical agents to break the bonds of the integral proteins with the cortex.

However, the actin cortex and the underlying cytoskeleton are dynamic structures. Functional and structural changes of the states of cells constantly demand local depolymerization of actin filaments in some cell regions and their local polymerization in the others. Besides that, local ruptures of the cortex or the underlying cytoskeleton can already occur at moderate loads or under the action of drugs. These mechanisms lead to local structural inhomogeneities of the membrane. They manifest themselves in the membrane's mechanical behavior since they give rise to a local decrease of its rigidity. We show here that such a local softening causes shape instabilities of the cell membrane in the form of spontaneous local deflections: blisters or invaginations. These instabilities are driven by a gradient of hydrostatic or osmotic pressure across the membrane. Please note that the threshold for deflection formation over such defects was observed in our micropipet experiments. In Sec. III A we show that this threshold can be explained by a local decrease in the membrane rigidity. If the pressure only slightly exceeds the threshold, the membrane possessing such a defect is deformed as a whole. However, far from the threshold the pressure becomes strong enough to overcome the attraction between bilayer and cortex, which results in the splitting of the compound membrane. This phenomenon is described in Sec. III B within a simple two-shell model.

A. The cell free energy and a general description of the local instability

In order to describe a local deflection of the membrane, one should take into account contributions to the membrane's elastic energy by describing the energetic cost of the bending, lateral stretching, and deformation of the bulk cytoskeleton [23]. To simplify the mathematical description, we consider an initially spherical cell with a radius R. The

free energy of an arbitrary distortion of the initial (spherical) shell shape can be expressed in the form [23]

$$F=\oint\{\tfrac{1}{2}(k\psi\Delta^2\psi+B\psi\Delta\psi+D_0\psi^2)+\tfrac{1}{3}a_3\psi^3+\tfrac{1}{4}a_4\psi^4\}dA, \tag{1}$$

where k is the membrane-bending elasticity modulus. The function $\psi=\psi(\theta,\varphi)$ denotes the shell displacement that is normal to the initial spherical surface of the membrane; θ and φ are the spherical angles, A is the membrane surface area, and Δ is the Laplace-Beltrami operator on the sphere. B and D are membrane parameters. They are functions of the pressure difference $p=p_{\rm out}-p_{\rm in}$, the spontaneous curvature c, the lateral compressibility modulus of the membrane λ, and Young's modulus $E_{\rm cyt}$ and Poisson's ratio $v_{\rm cyt}$ of the bulk cytoskeleton:

$$B=\frac{pR}{2}+\frac{k(2+cR)}{R^2},\quad D_0=\frac{p}{R}+\frac{2kc}{R^3}+\frac{4\lambda}{R^2}+\frac{E_{\rm cyt}}{(1-2v_{\rm cyt})R}.$$

The first term of Eq. (1) describes the bending elasticity of the membrane. The second term in Eq. (1) describes the energy contribution due to the change of the membrane surface area. The first item in B represents the well-known Laplace expression for the tension of a spherical surface radius R subjected to the osmotic pressure difference p. The second describes the contribution of the bending elasticity playing the role of the surface tension. Hence the parameter B from the second term of Eq. (1) should be considered the effective surface-tension coefficient of the membrane. Finally, the third term of Eq. (1) describes the membrane energy that is proportional to the square of the displacement, ψ. Therefore it is analogous to the conventional Hook's law, with the parameter D playing the role of an effective spring constant of the membrane (with respect to the normal displacement). Several effects, such as the osmotic pressure difference (the first item), the bending elasticity (the second item), the lateral compressibility modulus (the third term), and the spring constant of the bulk cytoskeleton (the last term of expression D) contribute to the effective spring constant D. The bending elasticity modulus k, the lateral compressibility modulus of the membrane λ, and the spontaneous curvature c are phenomenological parameters characterizing mechanical properties of the composite membrane as a whole, rather than of some of its constituents.

Several different phenomena contribute to nonlinear terms of the free-energy expression that are characterized by the coefficients a_3 and a_4. Their detailed discussion is beyond the scope of this paper, and we therefore consider a_3 and a_4 as phenomenological parameters, with a_4 always positive while a_3 can have either sign. Note that in the case of a homogeneous shell, the parameters a_3 and a_4 are constants. In contrast, in the vicinity of an inhomogeneity they may depend on coordinates: $a_{3,4}=a_{3,4}(\mathbf{R})$. A detailed derivation of the free energy (1) describing a local deformation of a spherical cell membrane can be found elsewhere [23].

The undisturbed spherical cell shape corresponds to the value $\psi=0$. Local softening of the membrane means that either the value of the lateral compressibility modulus λ or the elasticity $E_{\rm cyt}$ of the bulk cytoskeleton in the vicinity of the membrane surface is decreased locally. Both cases result in a lateral dependence of the parameter $D_0=(\theta,\varphi)$, which can be expressed as $D_0(\theta,\varphi)=D-U(\theta,\varphi)$, where D is a constant. The variation of the parameter D_0 with the surface coordinates is taken into account by introducing the function $U(\theta,\varphi)>0$, which describes the local softening. In the following, $U(\theta,\varphi)$ is referred to as ''the softening function.'' This function exhibits a maximum value in the region of softening and decays to zero outside this region. In the following, we consider soft regions whose widths are much smaller than the cell radius R. One can see that in the case of actin-filled vesicles, the function $U(\theta,\varphi)$ is proportional to the decrease of the F-actin concentration in the defects of the cortex in such a way that the integral $\oint U(\mathbf{R})dA$ is proportional to the decrease in the amount of filamentous actin side the soft regions. In the case of a cell softening, variations of the parameter D can arise either from a local softening of the actin cortex (i.e., related to the local decrease of the lateral compressibility modulus λ) or from a local softening of the underlying cytoskeleton (i.e., caused by the local decrease of $E_{\rm cyt}$). In either case the softening function is related to the decrease of the actin concentration or the cross-linker density in the soft region of the cortex or of the cytoskeleton.

Variation of the energy F yields the following equation of shape equilibrium:

$$k\Delta^2\psi+B\Delta\psi+D\psi-U(\mathbf{R})\psi+a_3\psi^2+a_4\psi^3=0. \tag{2}$$

Equation (2) has the trivial solution $\psi=0$ describing the spherical cell shape. However, under certain conditions this solution becomes unstable and a nontrivial solution $\psi(\mathbf{R})\neq 0$ arises, which describes a nonspherical cell shape. In order to study the instability threshold, consider an auxiliary eigenvalue equation obtained by the linearization of Eq. (2) in the vicinity of its trivial solution:

$$k\Delta^2 v_n+B\Delta v_n-U(\mathbf{R})v_n=\Lambda_n v_n, \tag{3}$$

where v_n are the eigenfunctions and Λ_n are the eigenvalues of the auxiliary equation enumerated by n that in general can take discrete and continuous values.

In the following, we outline a possible solution of Eq. (2) and study general properties of the phenomena, providing Λ_n and v_n have been found. In order to show that such solutions exist, we then give exact solutions of Eq. (3) for several softening functions.

Assume that Eq. (3) possesses a discrete spectrum, or that at least a part of the spectrum is discrete and that we have found the eigenvalues Λ_n ($n=1,2,3,\ldots$; $\Lambda_1<\Lambda_2<\ldots$) of the discrete part of the spectrum and the corresponding eigenfunctions $v_n(\mathbf{R})$.

A solution of Eq. (2) can be found by evoking the theory of branching of nonlinear equations [24]. This theory predicts that as soon as the parameter D of Eq. (2) becomes equal to the first eigenvalue Λ_1 of the auxiliary equation (3), the trivial solution $\psi=0$ becomes unstable. Denote this critical value of the parameter D as $D^*=\Lambda_1(B,k)$. One can consider this spectral condition as an implicit relation that determines the critical values of internal cell parameters (as,

for example, the critical value p^* of the osmotic pressure) leading to the instability of the spherical cell shape.

Assume now that the eigenfunction $v_1(\mathbf{R})$ and the corresponding eigenvalue Λ_1 of the auxiliary equation (3) have been found. As soon as the parameter D becomes smaller than $D^*=\Lambda_1$ the solution $\psi(\mathbf{R})\neq 0$ branches off the trivial solution $\psi=0$. The main term of $\psi(\mathbf{R})$ has the form

$$\psi(\mathbf{R})=\xi v_1(\mathbf{R})+O(\xi^2) \tag{4}$$

[24], where ξ is the amplitude of the local deflection. The absolute value of the amplitude ξ is assumed to be small. It will be determined in such a way that the expression Eq. (4) gives an asymptotically exact solution of Eq. (2) [24] describing the equilibrium cell shape. The dependence of the solution (4) on spherical coordinates θ and φ is described by the eigenfunction $v_1(\mathbf{R})\equiv v_1(\theta,\varphi)$, which we assume to know. Substituting the solution (4) into the free-energy functional (1) yields

$$F(\xi)=\tfrac{1}{2}\varepsilon V_2\xi^2+\tfrac{1}{3}V_3\overline{a_3}\xi^3+\tfrac{1}{4}V_4\overline{a_4}\xi^4, \tag{5}$$

with $V_n=\int\{v_1(\mathbf{R})\}^n dA$ $(n=2,3,4)$, $\overline{a_m}=V_m^{-1}\int a_m(\mathbf{R})\{v_1(\mathbf{R})\}^m dA$, with $m=3,4$ and $\varepsilon=D-\Lambda_1$. The expression for $\overline{a_m}$ takes into account that in general the phenomenological parameters a_3 and a_4 may possess some dependence on coordinates in the soft region of the actin cortex. If this dependence can be neglected, one finds $\overline{a_m}\equiv a_m$.

Thus the problem is reduced to the investigation of the simple function $F(\xi)$ [Eq. (5)], the coefficients of which are independent of the coordinates. Though the constants V_n and $\overline{a_m}$ are still unknown, the simple structure of the free energy $F(\xi)$ makes it possible to describe some general properties of the bifurcation. From the mathematical point of view, the problem is analogous to that of a description of a phase transition within the Landau theory, namely to the case when the symmetry allows for the existence of a cubic invariant [25]. The amplitude ξ plays a role analogous to that of the order parameter. The equilibrium state corresponds to a global minimum of the free energy $F(\xi)$, Eq. (5). Minimization of the free energy is described in Appendix A. This analysis shows the following. The equation of equilibrium $\partial F/\partial\xi=0$ has the trivial solution $\xi=0$. This solution describes the cell without any blister or invagination. It corresponds to the global free-energy minimum (and hence to the equilibrium state) at $\varepsilon>\varepsilon_b$. Here

$$\varepsilon_b=\frac{2\overline{a_3^2}}{9\overline{a_4}}\frac{V_3^2}{V_2V_4} \tag{6}$$

is the value corresponding to the bifurcation point. At $\varepsilon\leqslant\varepsilon_b$, one of the two nontrivial solutions,

$$\xi=\frac{-\overline{a}_3V_3\pm\sqrt{\overline{a}_3^2V_3^2-4V_2V_4\overline{a}_4\varepsilon}}{2V_4\overline{a}_4}, \tag{7}$$

corresponds to the equilibrium state. In order to obtain the global minimum of the free energy, one must choose in Eq. (7) the ''+'' sign if $\overline{a}_3<0$ and the ''−''sign if otherwise. If

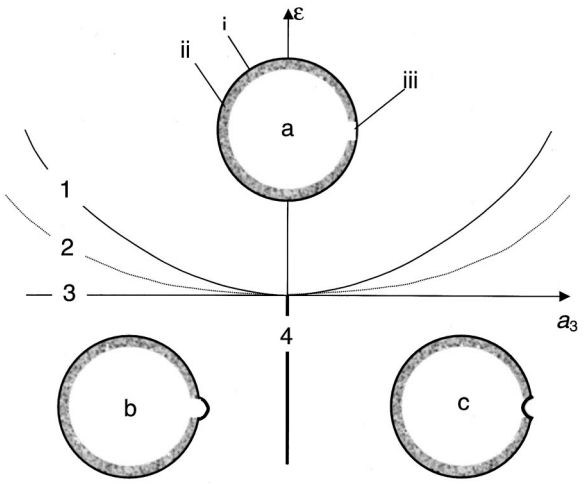

FIG. 6. Diagram of the membrane shape bifurcation driven by the local softening of the actin network. The bifurcation diagram separates the plane of the parameters ε and $\overline{a_3}$ into the parts where different cell shapes take place. Above line 1 the cell possesses no blister or invagination. The region of coexistence of a spherical state of the membrane and a state with blister or invagination resides between lines 1 and 3. The energy of a spherical membrane is equal to that of a membrane with a blister or an invagination on line 2. Below line 3 the cell inevitably possesses a blister or an invagination. In the right-hand part of the phase diagram ($a_3>0$, below line 2) the membrane has an invagination, whereas in the left-hand part ($a_3<0$, below line 2) it possesses a blister. The transition from blister to invagination occurs along line 4 ($a_3=0$, $\varepsilon\leqslant 0$). The only point on the phase diagram in which the bifurcation is soft is $\varepsilon=a_3=0$. Figures (a)–(c) give a schematic view of the membrane. (a) Initially spherical membrane containing the soft region in the actin cortex [(i) the lipid bilayer; (ii) the actin cortex; (iii) the soft region in the actin cortex]. (b) The cell with the blister localized over the soft region. (c) The cell with the invagination.

$\xi>0$ $(\overline{a}_3<0)$ of the amplitude (7) describes the blister; the case $\xi<0$ $(\overline{a}_3>0)$ corresponds to the invagination. One can break the plane $(\varepsilon,\overline{a_3})$ into parts where the free energy, Eq. (5), has different minima—this yields the bifurcation diagram. It is shown in Fig. 6. The detailed analysis and description of the bifurcation diagram is given in Appendix A.

Thus we have shown that if Eq. (3) has a nontrivial solution for a softening function $U(\mathbf{R})$, the local shape instability arises at $D=D^*$. However, we do not have any information concerning the exact form of $U(\mathbf{R})$. Moreover, it depends on the form of the softening function if Eq. (3) has a nontrivial solution. Therefore it is important to verify that Eq. (3) has a nontrivial solution corresponding to a discrete spectrum, at least for some functions of softening. This can be done by exactly solving Eq. (3) for several different reasonable functions of softening. There exists, however, an important case allowing for a universal consideration: a highly localized soft region. (The condition determining localization of the soft region is specified in Appendix D). If the soft region is localized in the vicinity of a point indicated by the angular coordinates θ_0 and φ_0 on the surface of the spherical cell, one can define the function of softening as

$$U(\theta,\varphi)=\frac{U_0}{R^2\sin\theta_0}\delta(\theta-\theta_0)\delta(\varphi-\varphi_0). \tag{8}$$

The details of the solution of Eq. (3) with the softening function (8) are discussed in Appendix B, where the exact solution is found yielding the eigenfunction in the following form:

$$v_1(\theta,\varphi)=\sum_{L=0}^{\infty}\frac{(2L+1)P_L(\mathbf{n}\cdot\mathbf{n}_0)}{kL^2(L+1)^2-BR^2L(L+1)+D^*R^4}, \quad (9)$$

where $\mathbf{n}$ is the normal vector with the spherical coordinates θ and φ, $\mathbf{n}_0$ is the one with θ_0 and φ_0, and $\mathbf{n}\cdot\mathbf{n}_0$ is their scalar product. $P_L(\mathbf{n}\cdot\mathbf{n}_0)$ is the Legendre polynomial.

The second important case is that of a thin elongated soft region. Consider a spherical cell whose membrane is softened in a thin region along the equator. The function of softening and the exact solution for the eigenvalue of Eq. (3) take the form

$$U=\frac{U_0}{2\pi R^2}\,\delta(\theta-\pi/2), \quad (10)$$

$$v_1(\theta)=\sum_{L=0}^{\infty}\frac{(2L+1)P_L(0)P_L(\cos\theta)}{kL^2(L+1)^2-BR^2L(L+1)+DR^4}. \quad (11)$$

The exact solutions of Eq. (3) for the eigenfunctions, Eqs. (9) and (11), make it possible to obtain the eigenvalue and, therefore, the instability threshold. In the case described by Eqs. (10) and (11), one finds

$$D^*=\tfrac{1}{4}\sqrt[3]{U_0^4/k}. \quad (12)$$

In the case where the soft region is located in the vicinity of a point, Eq. (8), one obtains

$$D^*=U_0^2/64k, \quad (13)$$

which gives the critical value of the osmotic pressure

$$p^*\approx\frac{U_0^2R}{64k}-\frac{4\lambda}{R}-\frac{E_{\mathrm{cyt}}}{1-2v_{\mathrm{cyt}}}-\frac{2kc}{R^2}. \quad (14)$$

The discussion of functions of softening and details concerning methods of obtaining exact and approximate solutions of Eq. (3) in different cases can be found in Appendixes C and D.

B. Description of the blister shape in the far overcritical regime

In the far overcritical regime, the above approach based on the expansions in series in terms of the amplitude cannot be applied. The shape of the blister is determined by a competition of bending energy, surface tension of the bilayer, and the work of the pressure difference. If the pressure rises extremely fast beyond the bifurcation point, the blister comes rapidly into the far overcritical regime, which results in bilayer cortex splitting. Consider this phenomenon, assuming that the membrane around the overcritical blister is approximately flat and represents the lipid bilayer shell that is locally split from the cortex. The latter is also a shell. Since it is much more rigid and does not support permanent pressure gradients, we neglect its deformation during the process. In this geometry the blister energy takes the form

$$F=\int\int\{\tfrac{1}{2}(k\psi\Delta^2\psi-\gamma\psi\Delta\psi)-p\psi\}dA, \quad (15)$$

where γ is the surface tension, whence it follows the equation describing the blister is

$$k\Delta^2\psi-\gamma\Delta\psi=p. \quad (16)$$

Assuming that the defect has a cylindrical symmetry, we look for a cylindrically symmetric solution with the boundary conditions $\xi=0$; $\partial\xi/\partial r=0$ at $r=R$, where R is the defect boundary radius. Since the cortex is much more rigid than the bilayer, the latter undergoes no vertical displacement at the rim $r=R$ of the defect. This is reflected by the first boundary condition. The second boundary condition ensures that the membrane remains smooth at the rim. The exact solution of Eq. (16) with the above boundary conditions takes the form

$$\psi=\frac{p}{4\gamma}\left\{2R\sqrt{\frac{k}{\gamma}}\,\frac{I_0\left(r\sqrt{\frac{\gamma}{k}}\right)-I_0\left(R\sqrt{\frac{\gamma}{k}}\right)}{I_1\left(R\sqrt{\frac{\gamma}{k}}\right)}+R^2-r^2\right\}, \quad (17)$$

where $I_{0,1}(z)$ are modified Bessel functions of the first kind.

Substitution of solution (17) into expression (15) yields the energy release during bending:

$$F=-\frac{\pi p^2R^4}{16\gamma}\left\{\frac{8k}{\gamma R^2}+1-4\sqrt{\frac{k}{\gamma R^2}}\,\frac{I_0\left(\sqrt{\frac{\gamma R^2}{k}}\right)}{I_1\left(\sqrt{\frac{\gamma R^2}{k}}\right)}\right\}. \quad (18)$$

As soon as the energy release is equal to the energy necessary to fracture bonds, $F+\pi R^2\sigma=0$, the splitting of the membrane from the cell body actually occurs. Here σ is the bond fracture energy per unit area. Therefore the condition of splitting takes the form

$$\sigma=\frac{p_{cr}^2R^2}{16\gamma}\left\{\frac{8k}{\gamma R^2}+1-4\sqrt{\frac{k}{\gamma R^2}}\,\frac{I_0\left(\sqrt{\frac{\gamma R^2}{k}}\right)}{I_1\left(\sqrt{\frac{\gamma R^2}{k}}\right)}\right\}, \quad (19)$$

where p_{cr} is the pressure difference that should be applied to a cell exhibiting a blister with the base radius R in order to increase the blister size by splitting the bilayer from the cortex. In the bending-dominated regime $\gamma R^2/k\ll 1$, the phenomenon is largely independent of the surface tension. In this case, expanding the Bessel functions in a power series one finds

$$F\approx-\frac{\pi p^2R^6}{384k}, \quad p_{cr}\approx\frac{8\sqrt{6k\sigma}}{R^2}. \quad (20)$$

In the tension-dominated regime $\gamma R^2/k\gg 1$, the energy gain and the condition of splitting take the form

$$F \approx -\frac{\pi p^2 R^4}{16\gamma}, \quad p_{cr} \approx \frac{4\sqrt{\gamma\sigma}}{R}. \tag{21}$$

IV. DISCUSSION

We provide experimental evidence for the shape changes of composite membranes composed of a lipid bilayer with associated actin networks in the form of blisters in areas where the actin cortex has a soft region or a hole. We show theoretically that a local softening of the cortex, or of the bulk cytoskeleton associated with the membrane, gives rise to a shape instability that is followed by the formation of blisters. This prediction could be verified for different experimental systems such as actin-filled vesicles and cells of the slime mold *Dictyostelium discoideum*. In the case of *Dictyostelium discoideum*, the actin cortex most likely possessed a hole that resulted in pressure-induced bleb formation. The presence of the hole in the cortex is suggested by the observation of organelles moving from the inner lumen of the cell into the blister. In the case of actin-filled vesicles, the soft regions are formed by slots between ''tectonic'' parts of the actin shell formed by self-assembly beneath the lipid bilayer. In this case, the soft regions should be considered as elongated ones. Our experimental findings together with the theoretical calculations presented here provide good evidence that local membrane shape instabilities can be driven by local softening of the cytoskeleton in different cells.

In the region where the actin network is weakened (or dissolved), the cell membrane is locally softened. This gives rise to pronounced local flickering. Such flickering was observed in the actin-filled vesicle [see Figs. 2(d) and 3(b)].

As pointed out above, there is an interesting toxicological case to be discussed in light of this theoretical analysis: the poisoning effect of phalloidin on the actomyosin system of hepatocytes (the main type of liver cells). In contrast to most other cell types, hepatocytes specifically take up phalloidin, an alcaloid from the poisonous fungus *Amanita phalloides* that binds very specifically to actin and induces the failure of bile flow (so-called cholestasis) in the living animal [26,27]. In the livers of rats treated with phalloidin, large cytoplasmic vacuoles derived from cell membranes are observed [28,29]. A similar effect was observed after the perfusion of isolated rat livers with cytochalasin B, another alkoloid interacting with actin [30]. In a primary cell culture, on the other hand, isolated hepatocytes develop plasma membrane blisters after phalloidin poisoning [31]. With specific antibodies it was also shown that the myosin was separated from the actin in the region of cell membrane protrusions of isolated phalloidin-treated hepatocytes [32]. Thus both cases—protrusions and invaginations of the plasma membrane—caused by a disturbance of the actin system have been observed with hepatocytes.

According to the above consideration, one can suppose that this is one of the leading mechanisms providing instability during phalloidin poisoning of these liver cells. Note that after the administration of phalloidin over a longer period (days), there is an increase of both actin and myosin observed in hepatocytes due to genetic induction of actin and myosin synthesis [33,34]. This is probably compensating for actomyosin dysfunction as has been shown by Loranger *et al.* [35], who also demonstrated a strong long-range increase of cytoplasmic keratin filaments. Since microtubuli are also supposed to play a role in the hepatocyte answer to phalloidin poisoning [36,37], the entire cytoskeleton in fact seems to be involved, yet on different time scales. The production of both protrusions and invaginations as an early event on the scale of minutes or hours can well be explained by the theory presented here. Consistent with the bifurcation in our mathematical model, the decision between inside or outside bending of the membrane could be brought about by differences in osmotic pressure across the membrane.

Recent studies of rat neurons have shown that local depolymerization of the actin cortex represents a necessary stage preceding axon formation [38]. In particular, it was concluded that local depolymerization of the actin cortex in a growth cone of a single neurite indicates that this is a neurite that will become an axon. Consistently, the absence of local actin depolymerization in a growth cone indicates that the latter will form a dendrite. Axon growth is driven by microtubules penetrating into distal areas of the growth cone through the defect [38]. Local actin depolymerization may give rise to the local shape instability (as described above) representing axon nucleation.

To summarize, we have observed local membrane shape changes (in the form of blisters) in the region of a local softening of the actin cortex of the slime mold *Dictyostelium discoideum* and in actin-filled vesicles. It is in agreement with previous observations with phalloidin-poisoned liver cells and reports on blebbing cells (cf the Introduction). We have shown theoretically that a local softening taking place in either the cortex or the bulk cytoskeleton adjacent to the membrane will necessarily initiate a shape instability that is followed by the formation of either blisters or invaginations (depending on the position in the phase diagram).

ACKNOWLEDGMENTS

This work was supported in part by the Deutsche Forschungsgemeinschaft via the Group Grant No. SFB 266. One of the authors, A. B., was supported by the Alexander von Humboldt Foundation and by the Deutsche Forschungsgemeinschaft via Grant No. SA 246/28-1.

APPENDIX A: PHASE DIAGRAM OF THE BIFURCATION

Minimization $\partial F/\partial \xi = 0$ of the free energy (5) with respect to the amplitude ξ gives the equation of equilibrium

$$\varepsilon V_2 \xi + V_3 \overline{a}_3 \xi^2 + V_4 \overline{a}_4 \xi^3 = 0. \tag{A1}$$

This equation has the trivial solution $\xi = 0$ and two nontrivial solutions [Eq. (7)]. Consider first the trivial solution. The condition $\partial^2 F(\xi)/\partial \xi^2 \geqslant 0$ with $\xi = 0$ yields the inequality $\varepsilon > 0$. Thus while $\varepsilon > 0$ (above line 3 in Fig. 6), the amplitude value $\xi = 0$ (describing the cell without blister or invagination) corresponds to the free-energy minimum. The same condition $\partial^2 F(\xi)/\partial \xi^2 \geqslant 0$ with the nontrivial solution [Eq. (7)] yields the inequality

$$\varepsilon \leqslant \frac{\overline{a}_3^2}{4\overline{a}_4} \frac{V_3^2}{V_2 V_4}. \tag{A2}$$

Note that due to the Cauchy-Bunyakovsky inequality, $V_3^2/V_2V_4<1$. Real nontrivial solutions of the equation of equilibrium (A1) exist under the condition (A2) (i.e., below line 1 in Fig. 6). The regions $\varepsilon>0$ and that described by (A2) are overlapping. In the domain of intersection $0\leqslant\varepsilon\leqslant\overline{a_3}^2V_3^2/4\overline{a_4}V_2V_4$ (between lines 1 and 3 in Fig. 6), the trivial and nontrivial solutions of Eq. (A1) coexist, both corresponding to free-energy minima. However, at $\varepsilon>\varepsilon_b$ (above line 2 in Fig. 6) the trivial solution corresponds to the more pronounced minimum of the free energy and hence to the equilibrium state. At $\varepsilon=\varepsilon_b$ (on line 2 in Fig. 6), the depth of the free-energy minimum corresponding to $\xi=0$ is equal to that corresponding to the nontrivial solution, Eq. (7). At $\varepsilon<\varepsilon_b$ (below line 2 in Fig. 6) the nontrivial solution corresponds to the more pronounced minimum. The cell membrane experiences thermal fluctuations. As soon as the minimum at $\xi\neq0$ becomes more pronounced than that at $\xi=0$, fluctuations provide the transition between the two states. Thus the bifurcation is determined by the equality of the free energies of the state with $\xi=0$ and that with $\xi\neq0$, Eq. (7): $F(0)=F(\xi\neq0)$, yielding the bifurcation condition Eq. (6) (line 2 in Fig. 6). Thus the solution $\xi=0$ is valid at $\varepsilon>\varepsilon_b$. In the bifurcation point $\varepsilon=\varepsilon_b$ (6), the equilibrium corresponds to the nontrivial solution (7), the amplitude ξ possessing a finite value $\delta\xi_0$:

$$\delta\xi_0=-\frac{2\overline{a_3}}{3\overline{a_4}}\frac{V_3}{V_4}. \tag{A3}$$

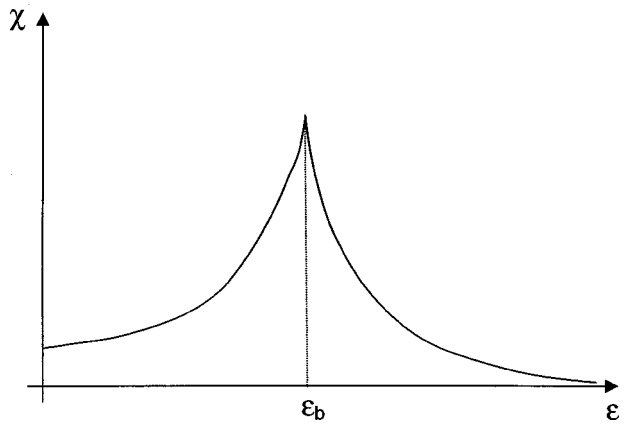

FIG. 7. Dependence of χ on ε.

The bifurcation is therefore analogous to a first-order phase transition close to second order.

Since $\overline{a_3}<0$ corresponds to the case of an invagination and $\overline{a_3}>0$ to that of a blister, the invagination-to-blister transition takes place under the condition $\overline{a_3}=0$, $\varepsilon<0$. In a special case, $\overline{a_3}=0$, the bifurcation is soft. In this case, the amplitude ξ continuously depends on ε: $\xi=0$ for $\varepsilon\geqslant0$ and $\xi_0{}^2=-\varepsilon V_2/\overline{a_4V_4}$ for $\varepsilon<0$. Thus on the plane $(\varepsilon,\overline{a_3})$, the condition $\varepsilon=\overline{a_3}=0$ determines the isolated point of the soft bifurcation.

The constant $\chi^{-1}=\partial^2F(\xi_0)/\partial\xi_0^2$ controlling the shape fluctuations takes the form

$$\chi^{-1}=\begin{cases}\varepsilon V_2, & \varepsilon\geqslant\varepsilon_b\\ \dfrac{\overline{a_3{}^2}V_3^2-4V_2V_4\overline{a_4{}^2}\varepsilon\mp\overline{a_3}V_3\sqrt{\overline{a_3{}^2}V_3^2-4V_2V_4\overline{a_4\varepsilon}}}{2\overline{a_4V_4}}, & \varepsilon<\varepsilon_b.\end{cases} \tag{A4}$$

The first branch of the constant χ ($\varepsilon\geqslant\varepsilon_b$) corresponds to the part of the bifurcation diagram above and the second one ($\varepsilon\leqslant\varepsilon_b$) to the part below line 2 (Fig. 6). The function $\chi=\chi(\varepsilon)$ is shown in Fig. 7.

APPENDIX B: EXACT SOLUTIONS OF THE AUXILIARY EQUATION IN THE CASE OF SOFT REGIONS IN A CORTEX LOCALIZED IN THE VICINITY OF A POINT AND THE EQUATOR OF A SPHERICAL CELL

The problem under consideration depends on two parameters with the dimension of length: l and d. The former is the size of the softened region. The latter has the physical sense of a cutoff distance at which the shell deflection caused by a local normal force vanishes [Fig. 1(b)]. The cutoff distance d is determined by elastic parameters of the shell: $d=(k/D)^{1/4}$ [23]. It is therefore independent of the defect size l. An estimate yields $d\sim10^{-7}$ m. If the size of the soft region l is much smaller than d ($l\ll d$), the soft region can be considered to be highly localized. In this case Eq. (3) can be solved exactly. The function of softening takes the form of Eq. (8). U_0 is the coefficient. The factor $U_0/R^2\sin\theta_0$ is chosen in such a way as to fulfill the condition $\oint U(\theta,\varphi)dA=U_0$. The spherical angles θ_0 and φ_0 fix the position of the soft region. One can expand the solution of Eq. (3) in a series in terms of spherical harmonics. The exact solution of Eq. (3) with the function of softening (8) takes the form

$$v_1(\theta,\varphi)=v_1(\theta_0,\varphi_0)\frac{U_0R^2}{4\pi}\times\sum_{L=0}^{\infty}\frac{(2L+1)P_L(\mathbf{n}\cdot\mathbf{n}_0)}{kL^2(L+1)^2-BR^2L(L+1)+D^*R^4}. \tag{B1}$$

$v_1(\theta_0,\varphi_0)$ is the value of the eigenfunction v_1 in the point of localization of the soft region that can be considered a normalizing constant. Choosing $v_1(\theta_0,\varphi_0)=4\pi U_0^{-1}R^{-2}$, one finds the eigenfunction, Eq. (9). In order to obtain the eigenvalue corresponding to the eigenfunction (B1), one can use

the following simple method. Taking $\theta=\theta_0$ and $\varphi=\varphi_0$ in the solution, Eq. (B1), one gets the equation

$$4\pi=U_0R^2\sum_{L=0}^{\infty}\frac{(2L+1)}{kL^2(L+1)^2-BR^2L(L+1)+D^*R^4}, \tag{B2}$$

which gives the eigenvalue $\Lambda_1=D^*$ of Eq. (3) in implicit form.

Consider the second important case of an elongated soft region allowing for an exact solution. Suppose that the actin cortex is softened along the equator of the spherical cell, forming a ''belt,'' so that the width of the softened area l is small ($l\ll d$). Following the same procedure, one obtains the eigenfunction

$$v_1(\theta)=\frac{U_0v_1(\pi/2)R^2}{4\pi}\times\sum_{L=0}^{\infty}\frac{(2L+1)P_L(0)P_L(\cos\theta)}{kL^2(L+1)^2-BR^2L(L+1)+DR^4} \tag{B3}$$

and the eigenvalue of Eq. (3) in the implicit form

$$4\pi=U_0R^2\sum_{L=0}^{\infty}\frac{(2L+1)P_L^2(0)}{kL^2(L+1)^2-BR^2L(L+1)+D^*R^4}. \tag{B4}$$

Here $v_1(\pi/2)$ is a normalizing factor. One can choose it as $v_1(\pi/2)=4\pi U_0^{-1}R^{-2}$ and obtain the eigenfunction (11). Note that since one finds $P_L(0)=0$ for odd L, there are only even terms in the expansions (B3) and (B4).

The exact solutions to Eqs. (B1) and (B2) and Eqs. (B3) and (B4) are important since these examples demonstrate that auxiliary equation (3) has nontrivial solutions, at least for the localized functions of softening, Eqs. (9) and (13). In these cases a discrete spectrum exists, and hence the local shape bifurcation takes place. The expressions for the eigenvalues and the eigenfunctions are, however, too cumbersome to be analyzed analytically. Thus it would be useful to find some approach making it possible to find approximate analytic solutions of the above problems (see Appendix C).

APPENDIX C: SOLUTION OF THE AUXILIARY EQUATION WITHIN A QUASIFLAT APPROXIMATION

Since the cutoff distance $d\sim10^{-7}$ m is much smaller than the cell size $R\sim10^{-5}$ m, one can approximately consider the problem as that on an infinite plane. The Laplace-Beltrami operator is approximately equal to the two-dimensional Laplace operator on a plane, $\Delta\approx\partial^2/\partial x^2+\partial^2/\partial y^2$, where x and y are the in-plane Cartesian coordinates. This approach is referred to as a quasiflat approximation. Also, estimations show that the inequality $k\Delta^2\psi\propto D\psi\gg B\Delta\psi$ is valid [23]. In this case, one can neglect the term $B\Delta\psi$ in the free energy (1) and in Eqs. (2) and (3). Within the quasiflat approximation one can write the auxiliary equation (3) on the plane (x,y) in the following form:

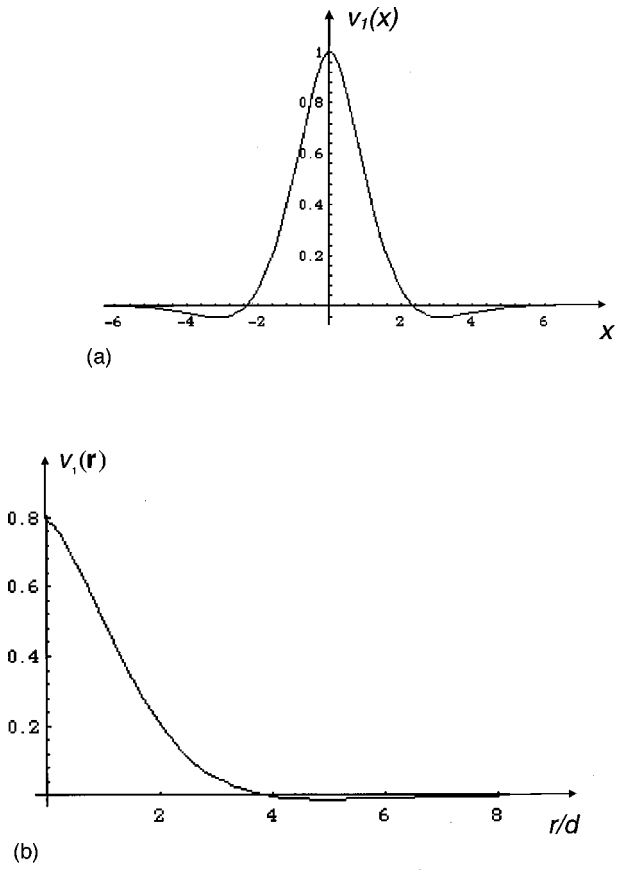

FIG. 8. The eigenfunctions v_1 describing the shapes of the blisters. The eigenfunctions are calculated in the quasiflat approximations: (a) the eigenfunction described by Eq. (C3) representing the shape of a blister above a narrow elongated soft region (cf the blisters Figs. 2 and 3), (b) the eigenfunction given by Eq. (C4) describing a blister above a soft region localized in the vicinity of a point.

$$k\Delta^2v_1-U(\mathbf{r})v_1=D^*v_1. \tag{C1}$$

Consider a highly localized elongated softened region in the framework of the quasiflat approximation. In this case one can express the function of softening in the form $U(x)=U_0\delta(x)$. One can try to find the solution of Eq. (C1) in terms of a Fourier expansion:

$$v_1(x)=U_0v_1(0)\int_{-\infty}^{\infty}\frac{\exp(iqx)}{kq^4+D}\frac{dq}{2\pi}. \tag{C2}$$

Taking $x=0$ in the expression (C2) and performing integration, one finds the eigenvalue Eq. (11). Choosing $v_1(0)=1$ and performing integration in Eq. (C2) one obtains the exact expression for the eigenfunction:

$$v_1(x)=\exp(-|x|/d\sqrt{2})\{\cos(x/d\sqrt{2})+\sin(|x|/d\sqrt{2})\}. \tag{C3}$$

Consider the soft region to be localized in the vicinity of the coordinate origin. In this case, one can express the function of softening as $U(\mathbf{r})=U_0\delta(\mathbf{r})$, where $\mathbf{r}=(x,y)$ is the in-plane radius vector. Applying the same procedure as the one above obtains the solution in the form of a Fourier integral: $v_1(\mathbf{r})=U_0v_1(0)\int\exp(i\mathbf{q}\cdot\mathbf{r})\{kq^4$

$+D(p^*)\}^{-1}d^2q/(2\pi)^2$. Taking $\mathbf{r}=0$, here one finds the eigenvalue Eq. (12) that gives the critical value of the osmotic pressure difference Eq. (13). Choosing the normalizing factor as $v_1(0)=2\pi/d^2$, one finds the solution for the eigenfunction

$$v_1(\mathbf{r})=-kei(r/d), \tag{C4}$$

where $kei(r/d)$ is the Kelvin function. The eigenfunctions (C3) and (C4), which describe the form of blisters in the corresponding cases, are shown in Fig. 8. Note that the form of the eigenfunction (C3) in Fig. 8(a) closely resembles the shape of the blisters that we observed in the actin-filled vesicles in Figs. 2 and 3.

Thus we have found a good approximation, making it possible to find simple solutions for the auxiliary equation in the cases of highly localized functions of softening. However, it would be useful to justify why this sort of solutions also exists for soft regions with finite sizes. In addition, one should show that the solutions corresponding to the functions of softening $\sim\delta(x)$ for highly localized soft regions can be obtained by way of a passage to the limit $l/d\to 0$.

APPENDIX D: SOLUTION OF THE AUXILIARY EQUATION IN THE CASE OF A SOFT REGION OF A FINITE SIZE

Consider a soft region in the actin cortex that has a finite size. Suppose that the cortex is softened along a curve whose curvature radius is much larger than the cutoff distance d. In this case, one can choose the coordinates in such a way that the y axis is directed along the softened region. The function of softening depends only on x: $U=U(x)$. Consider the simplest function of softening with the finite size l:

$$U(x)=\begin{cases} U_0/2l, & -l\leqslant x\leqslant l \\ 0, & x<-l; \qquad x>l. \end{cases} \tag{D1}$$

One can prove that if $U_0/2Dl>1$, the solution of Eq. (3) with the function of softening [Eq. (D1)] exists. The relation $U_0/2Dl>1$ can be valid for negative values of the osmotic pressure p. The solution takes the form

$$v_1(x)=\begin{cases} \exp(-|x|/d\sqrt{2})[C_1\cos(x/d\sqrt{2})+C_2\sin(|x|/d\sqrt{2})], & x\leqslant -l, \qquad x\geqslant l \\ C_3ch(\zeta x)+C_4\cos(\zeta x), & -l\leqslant x\leqslant l, \end{cases} \tag{D2}$$

where $\xi=2\sqrt{2}(U_0/2Dl-1)/d$. C_i are the coefficients. The function $v_1(x)$ and its first, second, and third derivatives must be continuous at the boundaries $x=\pm l$ of the soft region. This condition gives a homogeneous system of equations for the coefficients C_1, C_2, C_3, and C_4. Its solvability requires the determinant of this system to be equal to zero. If it is fulfilled, any three of these coefficients can be expressed in terms of the fourth. The latter is an arbitrary one, which, for reasons of simplicity, can be chosen to be equal to 1. The solvability condition is the equation whose solution gives the spectrum in the implicit form. With a good approximation, the eigenvalue takes the form

$$D^*\approx 0.11U_0^{5/4}(2kl)^{-1/4}+0.37U_0^{3/2}l^{1/2}(2k)^{-1/2}. \tag{D3}$$

The highly localized soft region can be considered as the limiting case of the finite-size soft region for $l/d\to 0$. The correspondence between the two functions of softening is fixed by the condition $\int_{-\infty}^{\infty}U(x)dx=U_0$. Note that for $l/d\to 0$ the solution (D3) gives $\sqrt[4]{64kD^3}/U_0\to 1$ and $C_1\to C_2$. This limit corresponds to the eigenvalue Eq. (11) obtained for the highly localized function of softening. This justifies the use of the highly localized function of softening in the form of the δ function. The solutions obtained justify that the existence of a soft region in the actin cortex gives rise to a shape instability of the membrane as soon as certain bifurcation conditions are met.

[1] S. J. Singer and G. L. Nicolson, Science **175**, 720 (1972).
[2] E. Sackmann, in *Structure and Dynamics of Membranes, From Cells to Vesicles*, edited by R. Lipowsky and E. Sackmann (North-Holland, Amsterdam, 1995), Vol. 1A, p. 1.
[3] A. Spudich and J. A. Spudich, J. Cell Biol. **82**, 212 (1979).
[4] T. P. Stossel, P. A. Janmey, and K. S. Zaner, in *Cytomechanics*, edited by J. Bereiter-Hahn, O. R. Anderson, and W. E. Reif (Springer-Verlag, Berlin, 1987), p. 883.
[5] D. Bray and J. G. White, Science **239**, 883 (1988).
[6] A. K. Harris, in *Biomechanics of Active Movement and Deformation of Cells*, edited by N. Akkas (Springer-Verlag, Berlin, 1990), p. 249.
[7] J. Condeelis, Annu. Rev. Cell Biol. **9**, 411 (1993).
[8] T. P. Stossel, Science **260**, 1086 (1993).
[9] H. Keller and P. Eggli, Cell Motil. Cytoskeleton **41**, 181 (1998).
[10] K. Schutz and H. Keller, Eur. J. Cell Biol. **77**, 100 (1998).
[11] C. C. Cunningham, J. B. Gorlin, D. J. Kwiatkowski, J. H. Hartwig, P. A. Janmey, H. R. Byers, and T. P. Stossel, Science **255**, 325 (1992).
[12] C. C. Cunningham, J. Cell Biol. **129**, 1589 (1995).
[13] A. Grebecki, Protoplasma **154**, 98 (1990).
[14] M. Yanai, C. M. Kenyon, J. P. Butler, P. T. Macklem, and S. M. Kelly, Cell Motil. Cytoskeleton **33**, 22 (1996).
[15] R. M. Hochmuth, J.-Y. Shao, J. Dai, and M. P. Sheetz, Biophys. J. **70**, 358 (1996).

[16] W. Häckl, M. Bärmann, and E. Sackmann, Phys. Rev. Lett. **80**, 1786 (1998).
[17] R. Grimm, M. Bärmann, W. Häckl, D. Typke, E. Sackmann, and W. Baumeister, Biophys. J. **72**, 482 (1997); M. Bärmann, W. Häckl, R. Grimm, S. Schrank-Kaufmann, I. Sprenger, and E. Sackmann (unpublished).
[18] J. Kas and E. Sackmann, Biophys. J. **60**, 825 (1991); K. Berndl, J. Kas, R. Lipowsky, E. Sackmann, and U. Seifert, Europhys. Lett. **13**, 659 (1990); U. Seifert, Phys. Rev. E **49**, 3124 (1994); U. Seifert and S. A. Langer, Europhys. Lett. **23**, 71 (1993); U. Seifert, Adv. Phys. **46**, 13 (1997).
[19] G. Gerisch, in *Current Topics in Developmental Biology* (Academic Press, New York, 1968), Vol. 3, p. 157.
[20] A. Spudich and J. A. Spudich, in *The Development of Dictyostelium Discoideum*, edited by W. F. Loomis (Academic Press, New York, 1982), p. 169.
[21] E. A. Evans, Methods Enzymol. **173**, 3 (1989).
[22] R. Simson, E. Wallraff, J. Faix, J. Niewöhner, G. Gerisch, and E. Sackmann, Biophys. J. **74**, 514 (1998).
[23] A. A. Boulbitch, Phys. Rev. E **57**, 2123 (1998).
[24] M. M. Vajnberg and V. A. Trenogin, *Theory of Branching of Solutions of Non-linear Equations* (Noordhoff International Publishing, Leyden, 1974).
[25] L. D. Landau, in *Collected Papers*, edited by D. Ter Haar (Pergamon, Oxford, 1965), p. 193; for more details on the case of Landau free energy with cubic invariants, see also J. C. Toledano and P. Toledano, *The Landau Theory of Phase Transitions* (World Scientific, Singapore, 1988); and Yu. M. Gufan, *Structural Phase Transitions* (Nauka, Moscow, 1982) (in Russian).
[26] M. Dubin, M. Maurice, G. Feldmann, and S. Ehlinger, Gastroenterology **75**, 450 (1978).
[27] M. Frimmer, Toxicol. Lett. **35**, 169 (1987).
[28] A. Lengsfeld and W. Jahn, Cytobiologie **9**, 391 (1974).
[29] B. Tuchweber, K. Kovacs, and K. Khandekar, J. Med. **4**, 327 (1973).
[30] W. Jahn, Naturwissenschaften **62**, 445 (1975).
[31] M. Frimmer, E. Petzinger, U. Rufeger, and L. B. Veil, Naunyn Schmiedebergs Arch. Pharmacol. **300**, 163 (1977).
[32] I. Nickola and M. Frimmer, Cell Tissue Res. **245**, 635 (1986).
[33] B. Tuchweber and G. Gabbiany, in *The Liver. Quantitative Aspects of Structure and Function*, edited by R. Preisig (Editio Cantor, Aulendorf, 1976), p. 84.
[34] S. Yasuura, T. Ueno, S. Watanabe, M. Hirose, and T. Namihisa, Gastroenterology **97**, 982 (1989).
[35] A. Loranger, B. Tuchweber, I. Youssef, and N. Marceau, Biochem. Cell Biol. **73**, 641 (1995).
[36] H. Kawahara and S. W. French, Am. J. Pathol. **136**, 521 (1990).
[37] N. Tsukada, C. A. Ackerley, and M. J. Phillips, Hepatology **21**, 1106 (1995).
[38] F. Bradke and C. G. Dotti, Science **238**, 1931 (1999).